Design and Testing of a Broadband Microstrip Line- Empty SIW Transition for 5G Applications

Anil Kumar Nayak, Vinit Singh Yadav, Amalendu Patnaik
Advanced Microwave Laboratory
Department of Electronics and Communication Engineering,
Indian Institute of Technology Roorkee,
Roorkee-247667, Uttarakhand, India.
Email: anayak@ieee.org; vyadav@ec.iitr.ac.in; apatnaik@ieee.org

***Abstract*—This paper presents a new broadband transition between microstrip and empty substrate integrated waveguide (ESIW) over 23-29 GHz band. In the proposed work, the design is initially implemented to use SIW and combined with three layers of the substrate such as top, bottom, and middle. One side without a cladding conductor and the other side just a conductor are implemented for the top and bottom layers. Simultaneously, the middle layer is used as air instead of the lossy dielectric to limit the loss. In order to improve matching, two shorting pins are placed on two sides of the middle layer. It can be found that the shorting pin's diameter and position plays a crucial role in providing broadband impedance bandwidth and low overall losses. Laboratory prototype of the structure is experimentally measured to validate the claim and the theoretical results. This transition finds suitable application for 5G communications.**

***Index Terms*—Broadband, Empty Substrate integrated waveguide, Impedance bandwidth, Overall losses.**

I. Introduction

Substrate integrated circuits (SICs) has brought over ample attention in the last two decades as it has a significant advantage and benefits for microwave and mm-wave applications. Consequently, substrate integrated waveguide (SIW) has some advantages than classical planar circuits, but also it has a few merits than traditional metallic rectangular waveguide (RW). The RW has some advantages so that people are still using it now, due to the low loss and high power handling capability. However, many issues have been noticed a traditional RW, such as size, weight, difficulties with active components, completely shielded, integration with planar structure, and more expensive. In order to overcome these issues, the SIW grabs more attention of researchers with many advantages. The beauty of the SIW is its low cost, compact size, lightweight. It does not have only some merits over RW and advantages over a microstrip line. It leads to the high quality (Q)-factor, easy fabrication and integration, more power handling capacity, and low loss than the MSL. However, the SIW have been used in microwave-, millimeter (mm) -, and Terahertz (THz) frequency ranges.

In 2006, the empty line, indeed SIW theoretical concept was first proposed in [1]. It was popularly known as modified-SIW (MSIW). The principle and operation of MSIW have been the same as the SIW, and is different if and only if the wave propagated primarily through the air medium. In 2014, the dielectric free SIW was reported in [2], popularly known as empty-SIW (ESIW). In the same year, two more research articles on the air-filled SIW (AFSIW) [3] and hollow-SIW (HSIW) [4] have been presented. The principle and operation of MSIW has been mostly the same as the AFSIW. From the manufacturing point of view, the AFSIW has been fabricated with simple conventional PCBs whereas the HSIW has been used for low-temperature cofired ceramic (LTCC) technology.

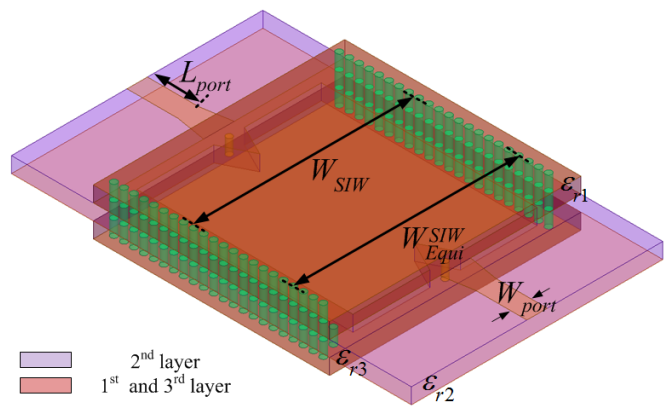

Fig. 1. Isomeric view the proposed design and detailed dimensions ($L_{port} = 5$, $W_{port} = 2$, $W^{SIW}_{Equi} = 22.029$; units: millimeters and $\varepsilon_{r1} = \varepsilon_{r2} = \varepsilon_{r3} = \varepsilon_r = 2.2$).

Recently, many works on ESIW with use of different techniques have been reported in [5]–[9]. In [5], the reconfigurable device has been used in the decoupled ESIW method. Consequently, it puts up with both electric and magnetic DC along with the biasing of liquid crystal. In order to solve off narrow-band and height issues, an intermediate guide concept has been used to overcome these two-issue, which has been presented in [6]. One of the many reasons to remove the dielectric an ESIW is to reduce the loss in the transition structure, which has been presented very well in [7]. In order to reduce the manufacturing complexity, a new through-wire microstrip -EISW transition has been proposed in [8]. Finally, a compact ultra-wide-band grounded-CPW to SIW transition along with flatter response of insertion loss has been reported in [9].

In this work, a broadband transition from the microstrip-to-

ESIW is designed, analyzed, and experimentally validated for the 5G application. This work's primary motivation is low loss, good impedance matching, and integration of the three-layer substrate because the multilayer provides the low loss and broadband impedance bandwidth. Here, an ESIW plays a very crucial role to reduce the insertion loss as the electromagnetic wave propagates through the air instead of the lossy dielectric. The proposed transition is designed, simulated, and verified experimentally from 23-29 GHz frequency range. This design reduces the insertion loss, improves the return loss, and provides broadband impedance bandwidth.

II. Transition Structures and Their Analysis

The design and analysis of broadband transition from microstrip to empty substrate integrated waveguide (ESIW) in the following steps (see Fig. 1 and 2).

1) Select the required frequency band and calculate the cutoff frequency (f_c), which is $1.25f_c - 1.9f_c$ for $TE_{10}-$mode
2) Select the length and width of the structure, which is length (L) and width (W).
3) Choose the value of diameter (d) of via and pitch (P) with respect to f_c.
4) Tune the tapered feed parameters (L_{tap} and W_{air}) to fix the dimensions of the design structure.
5) Also, tune the shorting pin position (L_{air}) and its diameter (d_{sp}) for better impedance matching.
6) Finally, to validate the simulated with the measured results.

An ESIW concept was reported first in 2014, by A. Belenguer *et* al. in [2]. The ESIW provide advantages like low loss, low posture, easy manufacturing, and integration in planar PCB. At the first stage, designer selects the f_c and overall dimensions of the structure, like length L and width W for a required band, which is helps to calculate the other dimension of the transition. In order to maintain the better impedance matching between microstrip and tapered line, we tune the length L_{tap} and W_{air} and then fixed it. Meanwhile,

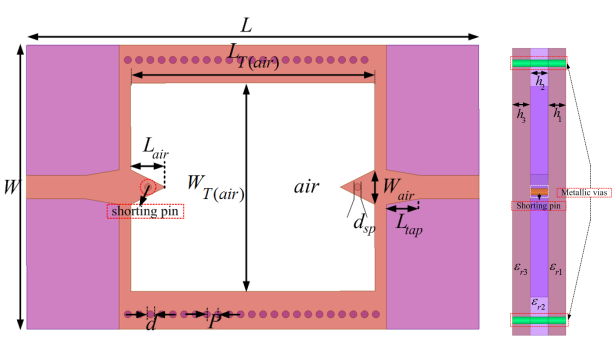

(a) (b)

Fig. 2. (a) Middle view (b) Side view of proposed transition ($d = 0.64$, $P = 0.975$, $d_{sp} = 0.3$, $W_{T(air)} = 18.029$, $L_{T(air)} = 12.309$, $W_{air} = 3$, $L_{tap} = 3$, $L_{air} = 3.2945$, $W = 24.589$, $L = 39.115$, $h = 1.524$; unit: millimeters).

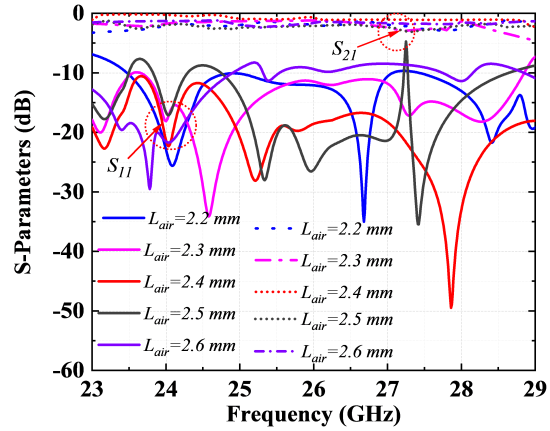

(a)

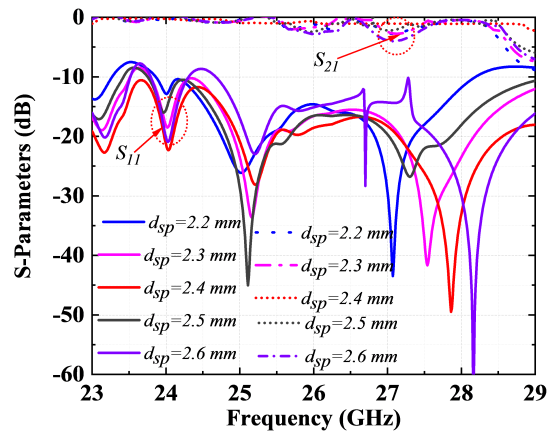

(b)

Fig. 3. S-parameters effect of (a) L_{air} and (b) d_{sp}.

the value of $L_{tap} = 3$ mm and $W_{air} = 3$ mm are fixed to maintain better matching. The pitch (P) and diameter (d) of vias are calculated in the second steps by using following equations:

$$\frac{\lambda_g}{5} \leq d \leq \frac{\lambda_g}{8}, P \leq 2d, \lambda_g = \frac{\lambda_0}{\sqrt{\varepsilon_{eff}}} \tag{1}$$

$$W_{SIW} = W_{Equi}^{SIW} - 1.08\frac{d^2}{P} + 0.1\frac{d^2}{W_{Equi}^{SIW}} \tag{2}$$

where W_{Equi}^{SIW} and W_{SIW} are the transverse and equivalent width of SIW cavity at TE_{10}-mode, respectively, and c is the velocity of light in free space. The λ_g and λ_0 are the guided wavelength and wavelength in free space, respectively.

The isomeric view of the proposed transition is shown in Fig. 1, whereas the middle and side view of this structure and its dimension is depicted in Fig. 2 (a) and (b), respectively. In order to achieve a low loss and broadband transition, the multilayer is one of the best options. Consequently, three substrate layers are used in this design in the starting. At the same time, the thickness of the top, middle, and bottom layers h_1, h_2, and h_3 are chosen, respectively. The thickness of each layer is fixed at 1.524 mm ($h_1 = h_2 = h_3 = h$) as per

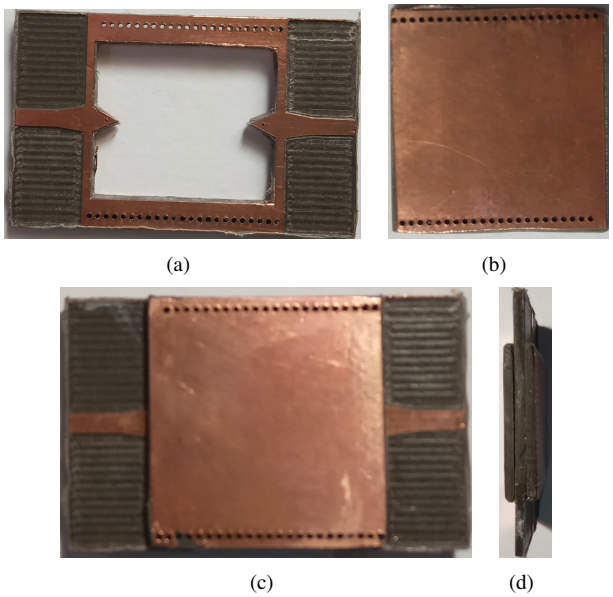

Fig. 4. The laboratory prototype of proposed design(a) Middle layer (air) (b) Top and bottom layer (c) Embedded of transition (d) Side view.

the availability of material. The top and bottom layers of the design, one side is etched with the copper cladding, i.e., only the substrate part, and the other one is kept on the copper sheet. These two layers are embedded in the middle layer. The middle layer is mostly combined with the rectangular-shaped airfield and feed section. This airfield's main objective is to reduce the insertion loss (*IL*) due to the electromagnetic wave propagating through the air instead of the lossy medium. In order to create artificial RW, the SIW technique is used in this structure. However, the P, d, and other dimensions are calculated using equations (1) and (2). Moreover, two taper shape structures are implemented in the middle layer, which is combined with the feed section at ports 1 and 2, respectively. As a result, the taper shape structures are playing a crucial role in improving the transition characteristics. The main two parameters of this taper are the position L_{air} of the shorting pin and its diameter d_{sp}. In order to fix the L_{air} and d_{sp}, we have used the parametric variation method. The parametric analysis effect of L_{air} and d_{sp} of the proposed structure analyzed, as shown in Fig. 3 (a) and (b). The RL is significantly surged as clearly shown in the plot. Whereas the maximum IL is found 0.79 dB from 24.5 to 29 GHz frequency range. Conversely, the IL is also found to be maximum 2.84 dB at lower band (23-24.5 GHz). At the end, the L_{air} is fixed at 3.2945 mm. Similarly, the variation of d_{sp} on the impedance matching and losses. Consequently, We have done parametric analysis and fix dimension of d_{sp} at 0.3 mm, which is depicted in Fig. 3 (b). This transition propagates the TE_{10} modes. The structure is designed on a single layer substrate, Rogers RT/duroid 5880 (TM) having a dielectric constant (ε_r) of 2.2, thickness (h) of 1.524 mm and loss tangent ($tan\delta$) of 0.0009. All the simulation carried out by using electromagnetic software ANSYS HFSS ver. 19.

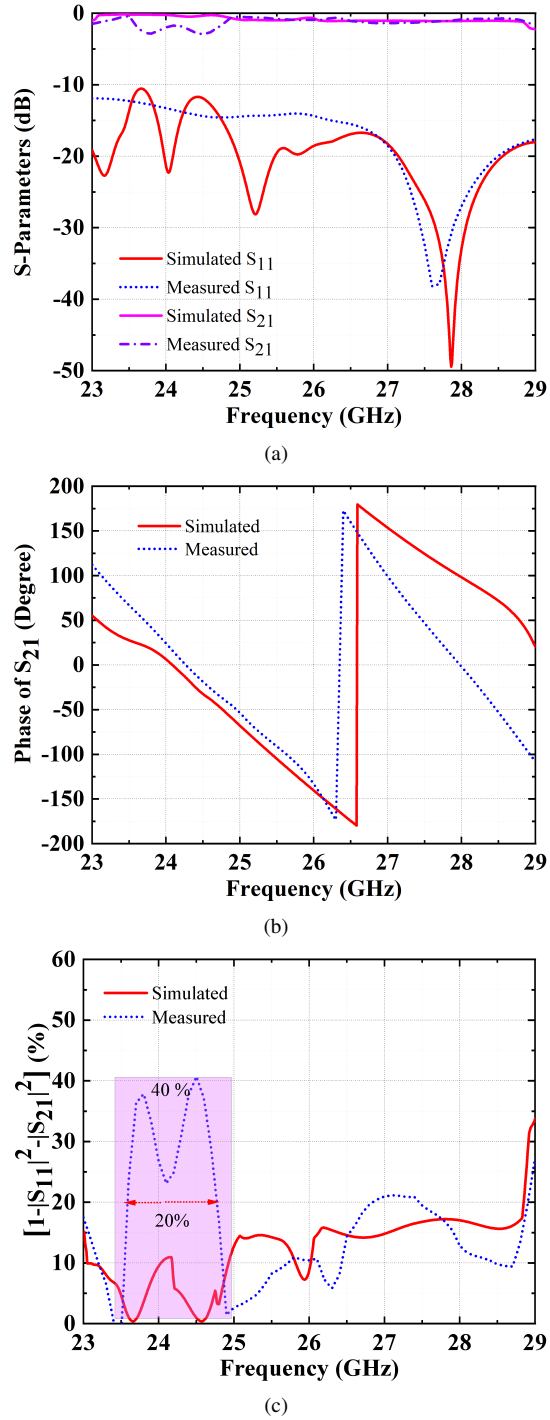

Fig. 5. Characteristics of the transition: (a) $|S_{11}|$ and $|S_{21}|$ (b) Phase of S_{21}, and (c) Total loss.

III. Experimental Validation

The laboratory prototype of the middle, top (same as the bottom) layers of the proposed transition are shown in Fig. 4 (a) and (b). Similarly, the integration of all three layers of PCB and side view of the laboratory prototype of design are depicted in Fig. 4 (c) and (d). The simulated and measured results $|S|-$parameters of the proposed transition is shown

Table I
COMPARISON OF COMPETITIVE TRANSITION DESIGNS BETWEEN MICROSTRIP AND ESIW

References	Frequency range M* (GHz)	RL (dB)	IL (dB)	BW (GHz)/ (%)	Type
[10]	8-20.5	11	1.5	12.5/87	RESIW
[11]	4-8	15	1.5	3.9/14.5	ESIW
This work	**23-29**	**12**	**0.82**	**6/23.07**	**ESIW**

M*=measured; **BW**=bandwidth

in Fig. 5 (a). The experimental results shows that the RL is above 15 dB (simulated: >15 dB) obtained and IL is below 0.82 dB (simulated:0.79 dB) achieved from 24.5 to 29 GHz frequency range. Similarly, the measured results of RL and IL are found greater than 12 dB (simulated: >12 dB) and less than 2.49 dB (simulated: <0.47 dB) from 23 to 24.5 GHz frequency range, respectively. From Fig. 5 (b), the phase of S_{21} is a significant parameter of the transition because most of the power is lost due to the time of filling of copper paste into vias in SIW. The measured and simulated results of the phase of S_{21} are shown in Fig. 5 (b). The measured and simulated results of the proposed transition's overall loss are matched as well, shown in Fig. 5 (c). It can be noticed that from Fig. 5 (c), the measured result of overall losses is found 20-40% between 23 to 24.5 GHz frequency range and below 20% in between 24.5 and 29 GHz frequency band. Finally, it has been observed that the measured result found in good agreement with the simulated one.

In the proposed work, the return loss is a little bit better than [10] and 3-dB less than [11], which is details are shown in Table I. However, the insertion loss has been found a little bit better than [10], [11]. Additionally, the measured bandwidth relatively higher than [10] and lesser than [11] from the proposed work.

IV. CONCLUSION

This paper presents a broadband transition between microstrip and EISW for mm-wave frequency range (23-29 GHz). The proposed transition has acceptable good return loss, low insertion loss, wider bandwidth, and better impedance matching in the whole passband. This transition is suitable for 5G applications in the mm-wave frequency range.

REFERENCES

[1] N. Ranjkesh and M. Shahabadi, "Reduction of dielectric losses in substrate integrated waveguide," *Electronics Letters*, vol. 42, no. 21, pp. 1230–1231, 2006.

[2] A. Belenguer, H. Esteban, and V. E. Boria, "Novel empty substrate integrated waveguide for high-performance microwave integrated circuits," *IEEE Transactions on Microwave Theory and Techniques*, vol. 62, no. 4, pp. 832–839, 2014.

[3] F. Parment, A. Ghiotto, T. Vuong, J. Duchamp, and K. Wu, "Broadband transition from dielectric-filled to air-filled substrate integrated waveguide for low loss and high power handling millimeter-wave substrate integrated circuits," in *2014 IEEE MTT-S International Microwave Symposium (IMS2014)*, 2014, pp. 1–3.

[4] L. Jin, R. M. A. Lee, and I. Robertson, "Analysis and design of a novel low-loss hollow substrate integrated waveguide," *IEEE Transactions on Microwave Theory and Techniques*, vol. 62, no. 8, pp. 1616–1624, 2014.

[5] J. R. SÃ¡nchez, C. Bachiller, V. Nova, and V. E. Boria, "Reconfigurable resonator in decoupled empty siw technology using liquid crystal material," *Electronics Letters*, vol. 55, no. 16, pp. 907–910, 2019.

[6] J. A. MartÃnez, A. Belenguer, J. J. De Dios, H. E. GonzÃ¡lez, and V. E. Boria, "Wideband transition for increased-height empty substrate integrated waveguide," *IEEE Access*, vol. 7, pp. 149 406–149 413, 2019.

[7] D. Herraiz, H. Esteban, J. A. MartÃnez, A. Belenguer, and V. Boria, "Microstrip to ridge empty substrate-integrated waveguide transition for broadband microwave applications," *IEEE Microwave and Wireless Components Letters*, vol. 30, no. 3, pp. 257–260, 2020.

[8] A. Belenguer, J. A. Ballesteros, M. D. Fernandez, H. E. GonzÃ¡lez, and V. E. Boria, "Versatile, error-tolerant, and easy to manufacture through-wire microstrip-to-esiw transition," *IEEE Transactions on Microwave Theory and Techniques*, vol. 68, no. 6, pp. 2243–2250, 2020.

[9] D. Lorente, M. Limbach, H. Esteban, and V. Boria, "Compact ultrawideband grounded coplanar waveguide to substrate integrated waveguide tapered v-slot transition," *IEEE Microwave and Wireless Components Letters*, pp. 1–4, 2020.

[10] D. Herraiz, H. Esteban, J. A. MartÃnez, A. Belenguer, and V. Boria, "Microstrip to ridge empty substrate-integrated waveguide transition for broadband microwave applications," *IEEE Microwave and Wireless Components Letters*, vol. 30, no. 3, pp. 257–260, 2020.

[11] Y. Ding and K. Wu, "Substrate integrated waveguide-to-microstrip transition in multilayer substrate," *IEEE Transactions on Microwave Theory and Techniques*, vol. 55, no. 12, pp. 2839–2844, 2007.